University Library

MINERVA ACCESS

A gateway to Melbourne's research publications

Minerva Access is the Institutional Repository of The University of Melbourne

Author/s:
Nathanael, JG;Kang, H;Wille, U

Title:
Exploring Substituted Dihydroxybenzenes as Urease Inhibitors through Structure–Activity Relationship Studies in Soil Incubations

Date:
2025-08

Citation:
Nathanael, J. G., Kang, H. & Wille, U. (2025). Exploring Substituted Dihydroxybenzenes as Urease Inhibitors through Structure–Activity Relationship Studies in Soil Incubations. ChemPlusChem, 90 (8), https://doi.org/10.1002/cplu.202500068.

Persistent Link:
https://hdl.handle.net/11343/367550

License:
CC BY-NC-ND

Research Article
doi.org/10.1002/cplu.202500068
Chemistry Europe
European Chemical Societies Publishing

www.chempluschem.org

Exploring Substituted Dihydroxybenzenes as Urease Inhibitors through Structure–Activity Relationship Studies in Soil Incubations

Joses G. Nathanael,* Haohan Kang, and Uta Wille

Urea fertilization as nitrogen (N) source is essential for increasing crop productivity. However, it results in significant N loss through ammonia volatilization, nitrate leaching, and nitrous oxide emissions, causing environmental harm and economic loss. Urease, an enzyme in soil, rapidly catalyzes urea hydrolysis to ammonia/ammonium. To reduce ammonia volatilization, urease inhibitors delay hydrolysis until urea is dissolved in the soil body. The commercial product *N*-(*n*-butyl)thiophosphoric triamide (NBPT) is effective only in certain soils, yet it dominates the current global urease inhibitor market. This study examines the performance of un- and substituted dihydroxybenzenes (DHBs) as alternatives to NBPT in two Australian soils. Among them, 4-fluorocatechol (DHB **6**) and 4-bromocatechol (DHB **8**) are more effective in delaying urea hydrolysis than NBPT in acidic sandy loam soil. Michaelis–Menten kinetics reveals that NBPT acts as a competitive inhibitor, while DHB **8** acts as a noncompetitive inhibitor. Density functional theory calculations suggest that DHB **8** binds to the cysteine residue in the urease mobile flap, reducing its flexibility and preventing it from assisting urea hydrolysis. This study demonstrates the potential of DHBs as efficient urease inhibitors in certain soils, offering an environmentally viable alternative to NBPT.

1. Introduction

Projections from the United Nations indicate that by the end of the 21st century the global population could reach nearly 11 billion,[1] making the provision of food an increasingly urgent challenge. The application of fertilizers to supply nutrients to soils is crucial to increase crop yields and productivity while helping to minimize the need for additional agricultural land.[2–4] According to the Food and Agriculture Organization of the United Nations, the use of nitrogen (N) fertilizers in agriculture is the highest compared to other primary plant nutrients, with ≈113 Mt of N applied worldwide in 2020 alone.[5] Despite the essential need of N for plant growth,[6,7] on average only 50% of the applied N is taken up by plants.[8,9] The remaining N is lost from the plant–soil system to the environment through ammonia (NH_3) volatilization, nitrate (NO_3^-) leaching, and denitrification, which produces the harmful nitrous oxide (N_2O).[10,11] These various N loss pathways not only present economic challenges for farmers (and consumers) but are also a threat for the environment and human health.[12] Most notably, deteriorating water quality, loss of biodiversity, and increased releases of the greenhouse gas N_2O has been attributed to these undesired N losses.[13] Furthermore, the increased emissions of NH_3 contribute to the rise in ambient fine particulate matter ($PM_{2.5}$), which poses serious health risks and has been linked to raising human mortality rates.[14–16]

The market of synthetic N fertilizers is dominated by urea due to its high nutrient content (46% N), representing ≈50% of global N fertilizer usage in 2021.[17] Moreover, the demand for urea is predicted to steadily increase by around 1.5% each year.[18] In soil, urea is rapidly hydrolyzed by the enzyme urease into ammonium (NH_4^+),[19,20] which can readily be taken up by plants.[21] However, urea hydrolysis causes a localized increase of soil pH, which promotes N losses through NH_3 volatilization.[22,23] This loss pathway is particularly relevant in the case of top-dressed urea, where hydrolysis can occur faster than its dissolution into the soil body. One strategy to reduce NH_3 volatilization is by amending urea with urease inhibitors (UIs). By slowing down urease activity, and hence giving urea time (a few days) to fully dissolve in the soil body, NH_3 loss to the atmosphere can be reduced.[24–26] In fact, Germany has mandated the use of UIs as a measure to mitigate NH_3 emissions from agricultural soils.[27]

Efforts to increase nitrogen use efficiencies through the inhibition of soil urease have been made for more than six decades, exploring the inhibitory potential of over 14,000 compounds or compound mixtures.[28] Metals, for example, ions of silver (Ag^+), mercury (Hg^{2+}), and copper (Cu^{2+}), have shown inhibitory properties against soil urease.[29,30] Organic compounds were also tested, including xanthates,[31] hydroxamic acids,[32,33] polyhydric phenols (such as hydroquinone and catechol) and quinones,[34,35] and phosphoramides and thiophosphoramides.[36,37] While some of these compound classes showed promises in slowing down

J. G. Nathanael, H. Kang, U. Wille
School of Chemistry
ARC Research Hub for Smart Fertilisers
The University of Melbourne
Parkville, Victoria 3010, Australia
E-mail: joses.nathanael@unimelb.edu.au

Supporting information for this article is available on the WWW under https://doi.org/10.1002/cplu.202500068

© 2025 The Author(s). ChemPlusChem published by Wiley-VCH GmbH. This is an open access article under the terms of the Creative Commons Attribution-NonCommercial-NoDerivs License, which permits use and distribution in any medium, provided the original work is properly cited, the use is non-commercial and no modifications or adaptations are made.

© 2025 The Author(s). ChemPlusChem published by Wiley-VCH GmbH

urea hydrolysis and reducing NH_3 emissions, only three UIs are currently commercially available (**Figure 1**): the market leader *N*-(*n*-butyl)thiophosphoric triamide (NBPT), *N*-(*n*-propyl)thiophosphoric triamide (NPPT), and *N*-(2-nitrophenyl)phosphoric triamide (2-NPT).[18]

All three compounds are urea analogues, which are believed to coordinate to the two Ni(II) centers in the active site of urease, preventing binding of urea.[38] NBPT has been shown to successfully reduce NH_3 volatilization by some 40–50%, depending on the climate and soil conditions.[24,39] In some cases, the reduction can be as high as 96% in the first week following application.[40] Unfortunately, the effectiveness of NBPT diminishes at increased temperatures and in acidic soils. For example, at a 0.01% (w/w) NBPT application rate, NH_3 volatilization was reported to be 6 times faster at 32 °C than at 18 °C after 6 days.[41] A field study revealed that NH_3 volatilization protection by NBPT lasted only 2–3 weeks in acidic soils compared to over 7 weeks in alkaline soils.[42] Similarly, a laboratory incubation study showed that NBPT slowed down urea hydrolysis at pH 8.2 five times more effectively than at pH 5.5.[43] While a decrease in soil organic–matter content was found to significantly correlate with increased inhibitory effectiveness of NBPT,[44] soil pH and high clay content appeared to contribute more to NBPT efficiency than soil organic–matter content.[45] Given that NH_3 emission abatement is an important cost-effective strategy for $PM_{2.5}$ mitigation,[46,47] there is a pressing need to develop new urease inhibitors especially for soils where NBPT fails to perform.

Of the many different compounds tested for inhibitory activities for soil urease, catechol (1,2-dihydroxybenzene) was reported to perform well in various neutral soils (pH = 6.5–7.3) inhibiting urease activity up to 77%.[34] Interestingly, while substituted *p*-benzoquinones have been studied in soils,[48] substituted derivatives of catechol have not been explored as potential UIs in soil. Recent enzymatic studies in the absence of soil suggest that catechol, unlike (thio)phosphoramides, inactivates urease by forming a covalent bond with the cysteine residue on the enzyme's mobile flap.[49,50] This bond formation reduces the flexibility of the flap, preventing it to change from an open to a closed state, which is required for histidine residues on the flap to assist in urea hydrolysis. However, while enzymatic studies could provide useful indications what compounds might have potential as UIs, they cannot predict performance in the complex soil matrix. Thus, to identify more efficient UIs in soils where NBPT does not work well, we have performed soil microcosm incubations in two different Australian soils using a series of differently substituted dihydroxybenzenes (DHBs) to explore how the substitution pattern affects inhibitory activity (**Figure 2**). The mode of inhibition of successful UIs was explored through Michaelis–Menten kinetics and density functional theory (DFT) calculations.

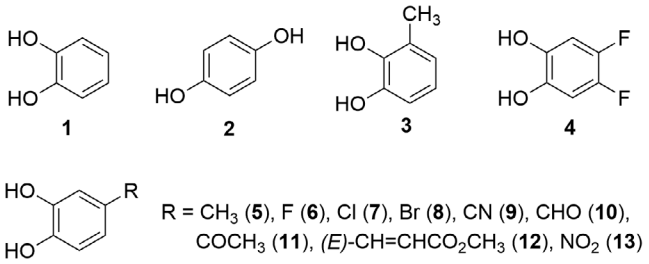

Figure 2. Dihydroxybenzenes (DHBs) studied in this work.

2. Experimental Section

2.1. Chemicals

DHBs **1**, **2**, **7**, and **13** were supplied by Sigma–Aldrich (Truganina, Victoria, Australia), DHBs **3**, **5**, and **9**–**11** were supplied by AKSci (Union City, CA, USA), DHB **4** was supplied by Aaron Chemicals (San Diego, CA, USA), DHB **6** was supplied by Enamine (Monmouth Junction, NJ, USA), and DHB **8** was supplied by Combi-Blocks (San Diego, CA, USA). DHB **12** was synthesized from caffeic acid, which was supplied by AKSci (Union City, CA, USA). The synthesis was carried out according to the literature procedure.[51] The synthetic procedure and spectroscopic data for DHB **12** are provided in the Supporting Information (SI). NBPT was supplied by Incitec Pivot Fertilisers (Geelong, Victoria, Australia) and used as positive control in all soil incubations. Potassium chloride (KCl) and phenylmercuric acetate (PMA), which were used in the soil extractions, were supplied by Merck (Bayswater, Victoria, Australia) and Sigma–Aldrich (Truganina, Victoria, Australia), respectively. For Michaelis–Menten kinetic experiment, Jack Bean Urease (JBU) and sodium nitroprusside were supplied by Sigma-Aldrich (Truganina, Victoria, Australia), while the rest of the chemicals were supplied by ChemSupply (Gillman, South Australia, Australia).

2.2. Site Description, Sampling, and Physiochemical Characterization

The soil was collected in March 2022 from two agricultural sites in Australia: a vegetable cropping soil from Tower Hill (THV) in Victoria, 38°20′19″S, 142°21′22″E; and a wheat cropping soil from Glenelg (GW) in New South Wales, 33°45′31″S,

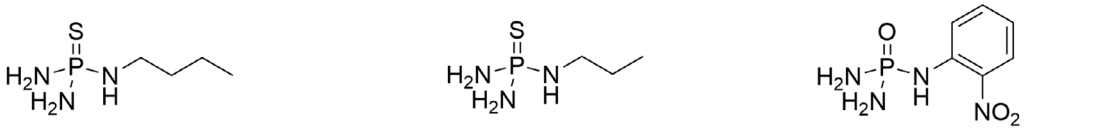

Figure 1. Current commercially available urease inhibitors.

© 2025 The Author(s). ChemPlusChem published by Wiley-VCH GmbH

148°06′52″E. The THV soil was classified as loam with a pH (1:5 $CaCl_2$) of 5.9 and the GW soil was classified as sandy loam with a pH (1:5 $CaCl_2$) of 4.4. Soil was collected up to 10 cm in depth from multiple spots throughout the site. Each soil type was homogenized to a composite sample, air-dried, ground, and passed through a 2 mm sieve to remove any plant residues and stones for the microcosm incubation experiments. Gravimetric water content was determined by oven drying at 105 °C for 24 h. Physical and chemical analysis of the soil properties was performed by Nutrient Advantage (Werribee, Victoria, Australia) (**Table 1**).

2.3. Soil Microcosm Incubation Experiments

A total of 20 g of air-dried and sieved (2 mm) soil was placed into a 250 mL polypropylene container (Sarstedt; Mawson Lakes, South Australia, Australia), wetted to 30–40% water-filled pore space (WFPS), and incubated at 25 °C for 1 week prior to the experiment to stabilize the microbial activity,[52] after which any lost water was replenished. The microcosm incubation experiment was set up with three replicates ($n = 3$), incorporating the following treatments: water control, urea, urea + NBPT, urea + DHBs. Urea was applied at 1000 mg N kg^{-1} dry soil as a solution in purified (Milli-Q) water. NBPT and DHBs were dissolved in the urea solution and applied at a rate of 0.25 mol% of applied N. Three milliliters of each treatment solution were applied to the soil to reach the final WFPS of 60%, which is the optimum value for microbial activity.[53] The containers were loosely closed to allow air exchange and incubated at 25 °C in the dark. During the incubation, the containers were aerated, and moisture was replenished as required (usually every week). The soils were destructively sampled at day 1 after treatment for the THV soil (incubation period limited due the high urease activity) and at days 0 (5 min), 3, 7, 10, and 13 after treatment for the less active GW soil.

2.4. Soil Mineral N and Urea Quantification

The destructive sampling was carried out to extract soil mineral N and urea by adding an aqueous KCl solution (2 M, 100 mL, 1:5 w/v), containing 10 mg L^{-1} of PMA (10 ppm), and shaking at 120 rpm for 1 h.[54] The suspension was filtered through a Whatman 42 filter paper (Interpath Services; Somerton, Victoria, Australia), and the filtrate stored at −20 °C until completion of the incubation experiment. Soil mineral N (NH_4^+-N and NO_3^--N, where the latter represents combined N from NO_2^- and NO_3^-) and urea concentrations from the extracts were determined using a Segmented Flow Analyzer (SAN++, Skalar, Breda, North Brabant, The Netherlands). The data for soil mineral N and urea are provided in the SI.

Table 1. Properties of the soils used in this study.

Soil property	Tower hill vegetable (THV)	Glenelg wheat (GW)
Location	38°20′19″S, 142°21′22″E	33°45′31″S, 148°06′52″E
Cation exchange capacity	36.9 C mol kg^{-1}	3.8 C mol kg^{-1}
pH (1:5 $CaCl_2$)	5.9	4.4
pH (1:5 water)	6.4	5.2
Organic carbon	49 g kg^{-1}	6.6 g kg^{-1}
NH_4^+-N	5.6 mg kg^{-1}	19 mg kg^{-1}
NO_3^--N	70 mg kg^{-1}	47 mg kg^{-1}
Sand (0.02–2 mm)	41.8%	69.4%
Silt (0.002–0.02 mm)	34.6%	17.5%
Clay (<0.002 mm)	23.6%	13.1%

2.5. Determination of the Rate of Urea Hydrolysis and the Percentage Urease Inhibition

Soil urea was extracted from 20 g air-dried soil using 2 M KCl solution as described above. The rate of urea hydrolysis was determined based on how much urea remained in the soil after a certain period of time, t (in days), according to Equation (1):

$$\text{Urea hydrolysis rate} = \frac{\Delta[\text{urea}]}{t} \quad (1)$$

where $\Delta[\text{urea}] = [\text{urea}]_{t=0} - \Delta[\text{urea}]_t$.

The percentage of urease inhibition was determined based on how much urea in the treated soils (UI) remained after a certain period of time, t, compared to the control (C) in the absence of inhibitor, according to Equation (2):

$$\%\text{Urease inhibition} = 100 - 100 \times \frac{\Delta[urea]_{UI}}{\Delta[\text{urea}]_C} \quad (2)$$

where $\Delta[\text{urea}]_{UI} = [urea]_{UI,t=0} - [\text{urea}]_{UI,t}$ and $\Delta[\text{urea}]_C = [\text{urea}]_{C,t=0} - \Delta[\text{urea}]_{C,t}$.

2.6. Michaelis–Menten Kinetics to Determine the Mode of Inhibition

Michaelis–Menten kinetics were studied by measuring the production of NH_4^+ under varying urea concentrations at constant concentrations of NBPT and DHB **8**. Buffer solution (K_2HPO_4 50 mM, EDTA 1 mM, LiCl 10 mM, pH = 8.2 ± 0.1) was prepared to dissolve JBU (0.02 U mL^{-1}), ammonium chloride (NH_4Cl, 10 mM stock solution), inhibitors (NBPT: 0.025 and 0.05 mM stock solution; DHB **8**: 0.005 and 0.01 mM stock solution), and urea (0.5, 1, 2, 5, 10, 20, 50, 100 mM stock solution). In a 96-well plate (Corning; Merck, Bayswater, Victoria, Australia), 40 μL of buffer or inhibitor solutions was added to 20 μL of JBU solution. The solutions were mixed thoroughly and preincubated in the dark for 5 min at 100 rpm and 25 °C using a digital shaker (Heathrow Scientific Digital Orbital Shaker, Scientifix, Clayton, Victoria, Australia). Then, 40 μL of urea stock solution (0.5, 1, 2, 5, 10, 20, 50, 100 mM) was added to each well (final [urea] in well: 0.2, 0.4, 0.8, 2, 4, 8, 20, 40 mM). In different wells, 100 μL of NH_4Cl solutions ([NH_4^+]: 0, 0.006, 0.01, 0.025, 0.05, 0.1, 0.25, 0.5 mM, each in triplicate) was added to obtain a standard curve for [NH_4^+]. The plate was incubated in the dark for 45 min at 25 °C. To determine the extent of urea hydrolysis, [NH_4^+] was measured colorimetrically according to a literature procedure.[55] For this, 50 μL of reagent A (phenol 1% w/v and sodium nitroprusside 0.03% w/v in the buffer solution) and 50 μL of reagent B (sodium

© 2025 The Author(s). ChemPlusChem published by Wiley-VCH GmbH

hydroxide 0.5% w/v and sodium hypochlorite 0.1% v/v in the buffer solution) were added to each well and the color was allowed to develop for 30 min at 37 °C. The absorbance was measured at 625 nm using a microplate reader (SPECTROstar Nano, BMG Labtech, Mornington, Victoria, Australia). According to the Beer–Lambert law, a standard calibration curve was constructed by plotting the optical density (OD) value against solutions with a known [NH_4^+]. This curve allows the [NH_4^+] in each well to be determined from its respective OD value. The amount of NH_4^+ generated over 45 min was plotted against the urea concentration to generate a hyperbolic curve where it reaches a maximum level as the urea concentration increases. Data analysis was performed with GraphPad Prism version 10.3.1 for Windows (GraphPad Software, Boston, Massachusetts, USA, www.graphpad.com), using nonlinear regression (curve fit) for Michaelis–Menten kinetics. The results used the best fit values with 95% likelihood. The Michaelis constant, K_m, represents the urea concentration, [urea], at which the reaction rate, υ, reaches 50% of its maximum rate, V_{max}, and serves as an inverse measure of the enzyme's affinity for the substrate, according to Equation (3).

$$\upsilon = \frac{V_{max}[\text{urea}]}{K_m + [\text{urea}]} \quad (3)$$

2.7. Statistical Analysis

Data are represented as the means of three or four biological replicates. Data were analyzed using analysis of variance (ANOVA) at $p < 0.05$ followed by the Fisher's least significant difference (LSD) test to compare treatment means in the GraphPad Prism version 10.3.1 for Windows (GraphPad Software, Boston, Massachusetts USA, www.graphpad.com). All results are reported as mean values ± standard error of the mean.

2.8. Computational Methods

DFT computations were carried out with the Gaussian 16 program[56] using the M062X method[57] in combination with the cc-pVTZ basis set,[58] using the conductor-like polarizable continuum model for water.[59] Dispersion corrections were performed using Grimme's GD3 method.[60] The ground and transition structures were verified by vibrational frequency analysis at the same level of theory, and all identified transition structures showed only one imaginary frequency. The Gaussian archive entries, including free energy data and imaginary frequencies of the transition state structures, are given in the SI.

3. Results and Discussion

3.1. Urea Hydrolysis Rate in Two Different Soils

We first explored the extent of urea hydrolysis over time. The THV soil had a high organic carbon content, which could be regarded as a proxy for a relatively high enzymatic activity.[61] Thus, due to the relatively fast urea hydrolysis, the percentage inhibition was determined after 24 h of incubation. On the other hand, the considerably lower organic carbon content in the GW soil enabled an extended incubation period to obtain a better time resolution, and the percentage of urease inhibition was determined 7 days posttreatment. The rate of urea hydrolysis and the percentage of urease inhibition for both soils are shown in **Table 2**.

Urea hydrolysis was significantly ($p < 0.05$) inhibited by the action of 11 of the tested compounds in the THV soil and 13 compounds in the GW soil. Except for NBPT, all compounds generally showed a better urease inhibition in the GW soil than in the THV soil. The finding for NBPT could be attributed to the high acidity of the GW soil ($pH_{CaCl2} = 4.4$), which is in line with previous studies that have reported a significant decline in NBPT effectiveness in acidic soils.[42,43] The known soil urease inhibitors, catechol (DHB **1**) and hydroquinone (DHB **2**), showed a moderate urease inhibition in the THV soil of about 30%. However, whereas the inhibitory activity of DHB **1** remains relatively unchanged in going to the more acidic GW soil, the effectiveness of DHB **2** increases to 66% in this soil. An electron-donating methyl substituent on catechol increases the inhibitory properties compared to the unsubstituted parent, particularly in the GW soil, with 3-methylcatechol (DHB **3**) being slightly more effective than 4-methylcatechol (DHB **5**). Overall, this finding is consistent with recent data from enzymatic studies where improved inhibition of bacterial urease from *Sporosarcina pasteurii* and plant urease from jack beans was observed in methyl catechols as opposed to catechol.[50] Interestingly, while all halogenated catechol derivatives (DHBs **4**, **6**–**8**) performed relatively poorly in the THV soil (7–26% urease

Table 2. Rate of urea hydrolysis and percentage of urease inhibition in two different soils.

Treatment[a]	Urea hydrolysis rate [mg urea hydrolyzed/kg soil/day]	
	Tower hill vegetable (THV) Soil[b]	Glenelg wheat (GW) soil[c]
Urea	1139 ± 25	194 ± 6
Urea + NBPT	391 ± 12 (66%)	107 ± 6 (45%)
Urea + DHB **1**	811 ± 27 (29%)	131 ± 9 (33%)
Urea + DHB **2**	787 ± 6 (31%)	66 ± 2 (66%)
Urea + DHB **3**	762 ± 31 (33%)	108 ± 4 (44%)
Urea + DHB **4**	1055 ± 14 (7%)	115 ± 1 (41%)
Urea + DHB **5**	800 ± 17 (30%)	119 ± 12 (39%)
Urea + DHB **6**	954 ± 12 (16%)	91 ± 7 (53%)
Urea + DHB **7**	842 ± 29 (26%)	85 ± 14 (56%)
Urea + DHB **8**	931 ± 28 (18%)	71 ± 5 (64%)
Urea + DHB **9**	1098 ± 20 (NI)[ns][d]	157 ± 3 (19%)
Urea + DHB **10**	1082 ± 4 (5%)	179 ± 1 (8%)
Urea + DHB **11**	1107 ± 8 (NI)[ns]	153 ± 2 (21%)
Urea + DHB **12**	1049 ± 22 (8%)	139 ± 5 (28%)
Urea + DHB **13**	1146 ± 16 (NI)[ns]	171 ± 4 (12%)[ns]

[a]Values are means ± standard error ($n = 3$). The value in brackets show the percentage of urease inhibition in different treatments, determined according to Equation (2); ns: not significant compared to the control treatment; [b]Soil extraction was performed 1 day after treatment; [c]Soil extraction was performed 7 days after treatment; [d]NI = no inhibition.

© 2025 The Author(s). ChemPlusChem published by Wiley-VCH GmbH

inhibition), in the GW soil these compounds inhibited urea hydrolysis as well as or even better than NBPT (41–64% urease inhibition). This is the first time that these halogenated catechols have been explored as urease inhibitors, and their promising performance in the acidic GW soil makes them excellent candidates to be explored in other acidic soils in the future. On the other hand, catechol derivatives possessing strongly electron-withdrawing substituents, such as cyano, carbonyl, carboxyl, and nitro groups (DHBs **9**–**13**), almost showed no inhibitory properties in the THV soil (<10%) and poor inhibitory performance in the GW soil (8–28%). It should be noted that the amount of NH_4^+ in soil at the end of the incubation generally reflected the urea hydrolysis rate, while the amount of NO_3^- remained relatively constant as no significant nitrification process was observed in this short period of time. Soil mineral N data from this extraction are shown in Table S1 and S2, Supporting Information.

3.2. Urea Profile in an Acidic Sandy Loam Soil

The percentage of urease inhibition shown in the previous section provides only a snapshot, as the data were derived from one timepoint. To obtain a more detailed picture, we determined concentration–time profiles of urea in the GW soil in the absence and presence of inhibitors. Soil extractions were performed on days 0, 3, 7, 10, and 13. A subset of DHBs studied in the previous section were explored, including the known UIs NBPT and hydroquinone (DHB **2**) and compared with a control incubation in the absence of UI (**Figure 3**).

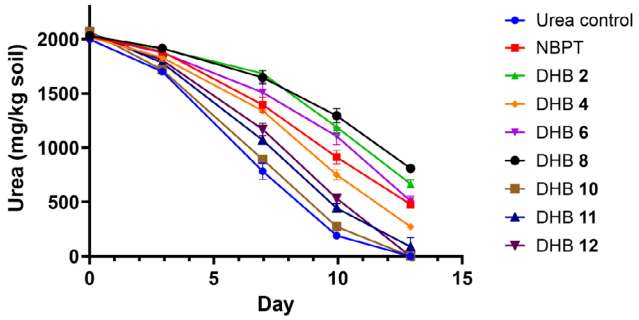

Figure 3. Urea profile in the GW soil over 13 days. Some error bars are to too small to be discernible.

The day 0 extraction was performed 5 minutes after the commencement of the soil treatment, resulting in a recovery of urea of more than 93%. In the absence of inhibitors, urea was completely hydrolyzed by day 13. Hydroquinone (DHB **2**) and the monofluorinated and monobrominated catechols (DHBs **6** and **8**), respectively, retained urea similarly or better than NBPT over the period of 2 weeks, with 4-bromocatechol (DHB **8**) emerging as the best inhibitor at the end of the incubation, even outperforming hydroquinone (DHB **2**). 4-Fluorocatechol (DHB **6**) was more efficient than NBPT in the first 10 days but ended up being as effective as NBPT on day 13. The inhibitory properties of 4,5-difluorocatechol (DHB **4**) were comparable to NBPT in the first week but diminished during the second week. Carbonyl-substituted catechol derivatives (DHBs **10** and **11**) and methyl caffeate (DHB **12**) exhibited very little urease inhibition that disappeared after day 10. These results are also reflected in the NH_4^+ profile over time where the best inhibitor, DHB **8**, has the slowest increase of NH_4^+ over the 2 week period (see Figure S1, Supporting Information). The urea and mineral-N data for this soil incubation are provided in Table S3, Supporting Information. It is important to point out that the aim is not to develop a UI that completely stops urea hydrolysis as urea is water soluble and can be washed out of the soil. As outlined in the introduction, the aim is to slow urease activity down for a couple of days after fertilizer application to the field to allow complete dissolution of urea in the soil body before hydrolysis occurs to reduce loss through NH_3 volatilization. On a different note, the results obtained in this 2 week soil incubation experiment reflect the results from the day 7 snapshot for the GW soil shown in Table 2. These findings show that the short-term soil incubation with just one time point is an appropriate screening method to identify compounds that can proceed to more time-consuming soil incubations and field studies.

3.3. Investigating the Mechanism of Inhibition

Michaelis–Menten kinetics were studied for the best performing inhibitor in the GW soil, 4-bromocatechol (DHB **8**), and the

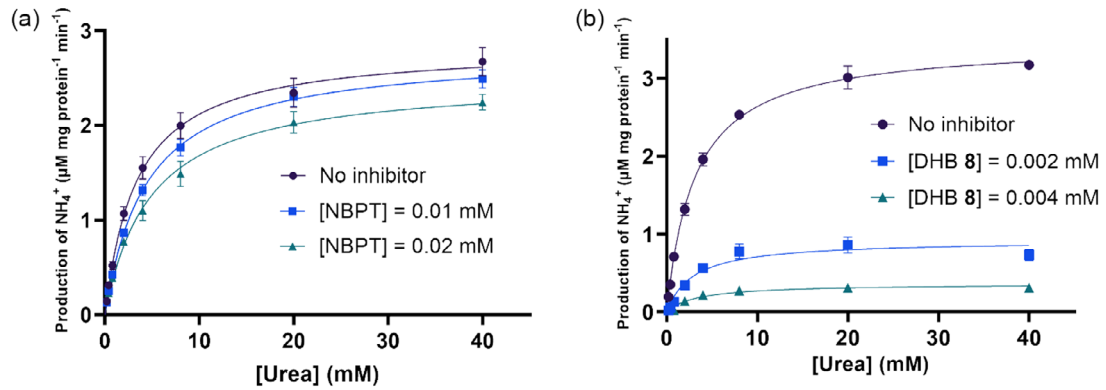

Figure 4. An exemplary Michaelis–Menten kinetic plot to show the effect of a) NBPT and b) DHB **8** on the NH_4^+ production. The incubations were performed with [urea] = 0.2, 0.4, 0.8, 2.0, 4.0, 8.0, 20, 40 mM in the buffer solution (pH = 8.2) at 25 °C for 45 min. Error bars are from standard deviations of three technical replicates.

© 2025 The Author(s). ChemPlusChem published by Wiley-VCH GmbH

commercial inhibitor NBPT using a JBU assay. The production of NH_4^+ in the absence and presence of inhibitors was plotted against the urea concentration. **Figure 4** shows an exemplary Michaelis–Menten kinetic plot for one of the biological replicates for both NBPT and DHB **8**, respectively. The other plots are provided in Figure S2 and S3, Supporting Information. The graph was fitted using nonlinear regression for Michaelis–Menten kinetics to obtain K_m and V_{max} (**Table 3**). It should be noted that because of the higher inhibitory activity of DHB **8**, its concentration was lower than that of NBPT.

The Michaelis–Menten plots showed saturation kinetics, where the NH_4^+ production became less affected by the urea concentration at higher [urea]. In the case of NBPT, V_{max} remained unchanged within experimental error ($p > 0.05$), whereas K_m increased with increasing [NBPT]. This behavior suggests that NBPT is a competitive inhibitor for JBU,[62] in agreement with previous findings.[63] On the other hand, compared to uninhibited enzymes, DHB **8** reduced V_{max} by about 55–80%, while K_m was unchanged within experimental error ($p > 0.05$). Based on this trend, DHB **8** inhibits JBU in a noncompetitive manner,[62] indicating that DHB **8** interacts differently with the active site in urease than urea and NBPT. This result corroborates previous findings which suggest that catechol binds to the mobile flap located at the outer end of the active site of urease, thereby preventing urea hydrolysis by reducing the flexibility of the flap.[49,50] It is highly likely that DHB **8** works in a similar manner.

Table 3. Michaelis–Menten kinetic parameters of the [urea]-dependent production of NH_4^+ by JBU in the absence and presence of NBPT and DHB 8, respectively, at two different concentrations.

Inhibitor[a]	Concentration [mM]	V_{max} [μM/mg protein min]	K_m [mM]
None[b]	–	2.5 ± 0.2	3.7 ± 0.2
NBPT	0.01	2.3 ± 0.3^{ns}	5.2 ± 0.6^{ns}
	0.02	2.1 ± 0.2^{ns}	7.2 ± 1.5*
None[c]	–	2.4 ± 0.5	3.4 ± 0.1
4-Bromocatechol (DHB 8)	0.002	1.1 ± 0.3*	3.0 ± 0.3^{ns}
	0.004	0.5 ± 0.2**	3.8 ± 0.6^{ns}

[a]Standard errors are errors of the mean calculated from four biological replicates (details in Table S4 and S5, Supporting Information). An ordinary one-way ANOVA was performed to assess the statistical significance of each inhibitor treatment compared to control (without inhibitor). Fisher's LSD post hoc tests were performed to compare inhibitor effects on V_{max} and K_m, statistical significance: ns = not significant, $p < 0.05$ (*), $p < 0.01$ (**); [b]Value determined from NBPT experiment; [c]Value determined from DHB **8** experiment.

3.4. Computational Studies of Possible Mechanism for Catechol Derivatives

In previous work by Mazzei et al.,[49,50] a mechanistic rationale was provided based on an X-ray analysis, which showed formation of the 3-*S*-adduct between catechol and the cysteine residue on the mobile flap. It was proposed that the reaction involves cysteinyl radicals, which could be formed through abstraction of the thiol-hydrogen by the semiquinone radical that results from one-electron oxidation of catechol (**Scheme 1**). Subsequently, the cysteinyl radical undergoes addition to catechol. The resulting radical adduct could be stabilized to form the closed-shell 3-S-product, for example, through reaction with oxygen.

However, given that the bond dissociation energy of a thiol S—H bond is higher than that of a phenolic O—H bond, i.e., MeS–H = 366 kJ mol^{-1},[64] catechol ≈330 kJ mol^{-1},[65] formation of the cysteinyl radical via hydrogen abstraction through semiquinone appears unfavorable. We therefore explored the mechanism of inhibition using DFT calculations using methyl thiol (MeSH) as a model system for cysteine, which confirmed that such hydrogen atom transfer is indeed endothermic by 12.7 kJ mol^{-1}. However, cysteinyl radicals can be obtained through alternative pathways given that one-electron oxidation of cysteine occurs readily in response to changes of the redox environment (E^0 cysteine/cystine = –0.22 V at pH 7).[66] To explore the feasibility of the proposed addition of cysteinyl radicals to catechol, we calculated the potential energy profile for this reaction (using MeS$^\cdot$ as model) in the presence of oxygen (**Figure 5**).

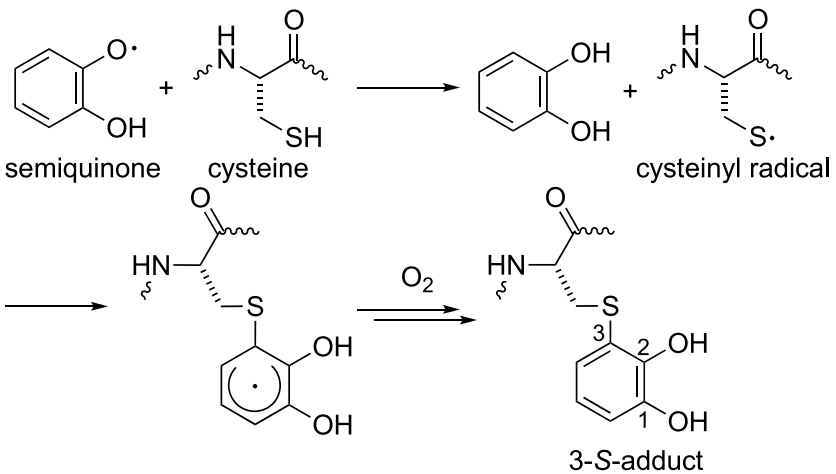

Scheme 1. Proposed mechanism for the reaction of cysteinyl radicals with catechol.[49,50]

© 2025 The Author(s). ChemPlusChem published by Wiley-VCH GmbH

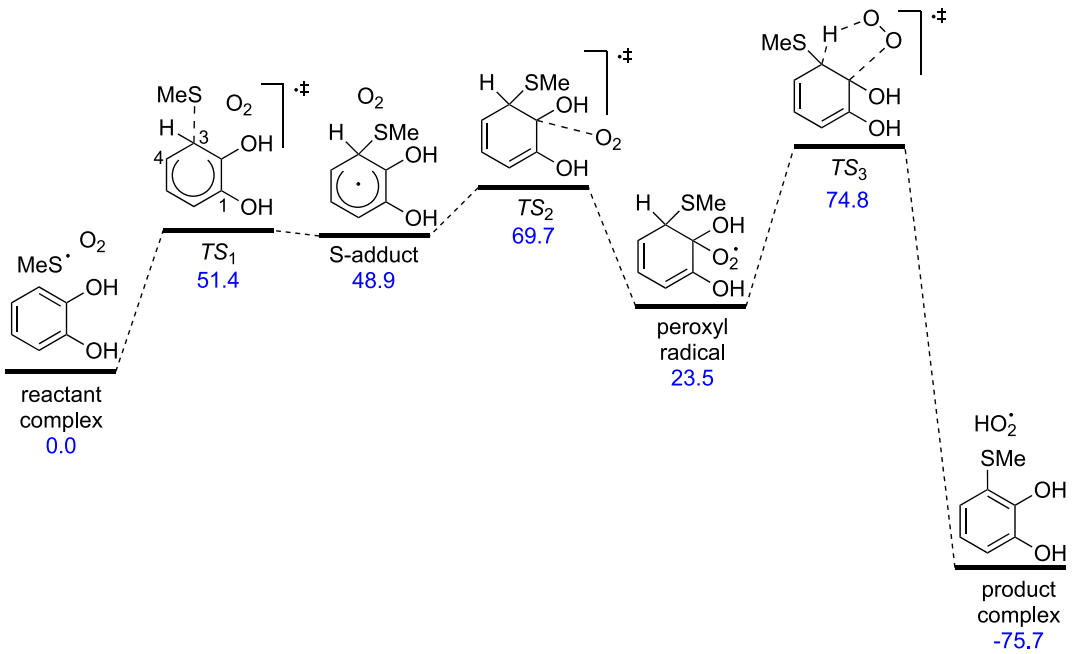

Figure 5. Potential energy surface for the reaction of MeS$^{\cdot}$ (as model for cysteinyl radicals) with catechol in the presence of O_2 (M062X(D3)/cc-pVTZ free energies in kJ mol^{-1}; using a solvation model for H_2O).

Interestingly, apart from the product complex all stationary points are energetically well above the reactant complex. The initial addition of MeS$^{\cdot}$ to catechol (the attack at *C*-3 shown here is energetically slightly more favorable by 2–3 kJ mol^{-1} than the attack at *C*-4) has a barrier of some 51 kJ mol^{-1} (TS_1), leading to the *S*-adduct, which is energetically just 2.5 kJ mol^{-1} below TS_1. Rearomatization through hydrogen abstraction by O_2 from the tetrahedral carbon to form $HO_2^{\cdot}$ is a two-step process, which

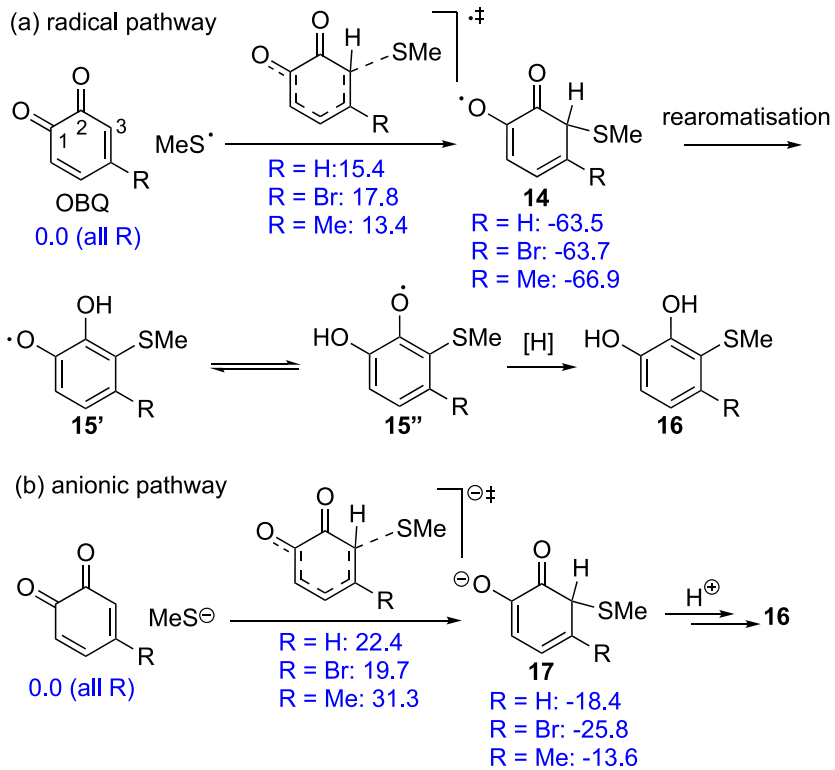

Scheme 2. Calculated energies for the addition of a) thiyl radicals or b) thiolate to OBQ (M062X(D3)/cc-pVTZ free energies in kJ mol^{-1}; using a solvation model for H_2O).

© 2025 The Author(s). ChemPlusChem published by Wiley-VCH GmbH

involves first O_2 addition via TS_2 to form a peroxyl radical, followed by loss of $HO_2^{\bullet}$ through a concerted five-membered transition state, which is associated with a barrier of some 50 kJ mol^{-1} relative to the peroxyl radical. While formation of the final product complex is exothermic by some 76 kJ mol^{-1}, the high energies associated with each stationary point on the energy surface make this entire process unlikely to proceed under environmental conditions.

What possible alternative mechanisms could occur? Given the ease by which catechol can be oxidized by soil metal oxides, even at low O_2 concentration,[67] it is not unreasonable to suggest that in situ formed *ortho*-benzoquinone (OBQ) is the actual active species. This proposal is supported by our finding that catechol derivatives that are inefficient as UIs, such as DHBs **9**–**13**, possess electron-withdrawing substituents, which should render their oxidation more difficult. OBQ is an excellent Michael acceptor, which could react with both radicals and anions.

Assuming formation of cysteinyl radicals (see above), **Scheme 2**a shows the energies associated with addition of MeS$^{\bullet}$ to unsubstituted, brominated, and methylated OBQ. While there are three positions where attack could occur, addition to *C*-3 is the energetically most feasible pathway (attack at the other positions is a few kJ mol^{-1} higher in energy, data not shown), in agreement with a recent experimental and computational study.[68] The data clearly show that radical addition is associated with a modest barrier of 13–18 kJ mol^{-1} in all cases and is considerably exothermic by at least 63 kJ mol^{-1}.

Transformation of the radical adduct to the thiol-substituted catechol proceeds via rearomatization to the semiquinone, followed by hydrogen transfer, which has been reported before.[68]

The pK_a value of cysteine in enzyme active sites can be lower by more than two units compared to the free amino acid,[69] and it is therefore possible that the cysteine residue on the mobile flap is deprotonated. The energies of the anionic pathway, while exothermic in all cases, are more dependent on the nature of the substituent (Scheme 2b). Thus, nucleophilic addition to the brominated OBQ at *C*-3 is kinetically and thermodynamically more favorable than to the methyl-substituted isomer with the energies for the unsubstituted OBQ lying in-between both.

While it is not possible to draw an unambiguous conclusion whether the reaction involves cysteine radicals or anions, the calculations strongly suggest that catechol and substituted derivatives do not act as UIs. Overall, either mechanism likely explains the excellent performance of DHB **8** in our 13 day soil incubations, whereas its poorer performance in the short-term studies could suggest that there was insufficient time for the oxidation to its OBQ derivative.

4. Conclusion

The soil incubation studies presented in this work enabled identification of three urease inhibitors, the known urease inhibitor hydroquinone (DHB **2**) and the new catechol derivatives 4-fluorocatechol (DHB **6**) and 4-bromocatechol (DHB **8**), that are more effective than the commercial inhibitor NBPT, particularly in the acidic GW soil. This is significant, given that NBPT is known to lose efficiency in acidic soils. In a 7 day incubation in the acidic GW soil, 3-methylcatechol (DHB **3**), 4,5-difluorocatechol (DHB **4**), and 4-chlorocatechol (DHB **7**) were also found to have a comparable inhibitory performance with NBPT.

Michaelis–Menten kinetic studies suggest that DHB **8** acts as a noncompetitive inhibitor, which likely reacts with the cysteine residue on the mobile flap through formation of a covalent bond. This mechanism is different from that of NBPT, which reversibly coordinates to the two Ni(II) centers in the active site.[70] Our findings suggest that catechol is oxidized in situ to OBQ, which acts as a Michael acceptor for either a cysteinyl radical or anion on the mobile flap in urease, ultimately resulting in a 3-*S* catechol adduct, which is in accordance with X-ray structures reported by Mazzei et al.[49,50]

This work highlights the potential of structure–activity relationship (SAR) studies in conjunction with mechanistic investigations to enable the discovery of new urease inhibitors. Having available a library of effective inhibitors for different soil types could potentially be a useful strategy to mitigate NH_3 emissions from agricultural systems. This approach can be considered as an extension to the 4R Nutrient Stewardship, which is using the right fertilizer source at the right rate, right time, and right place.[71] In future work, we will extend our SAR-based urease inhibitor development with special emphasis on exploring soils with properties where NBPT does not perform well.

Acknowledgements

The authors thank Deli Chen, Shu Kee Lam, and Helen Suter for helpful discussions. Supports by the Melbourne TrACEES Platform (Trace Analysis for Chemical, Earth and Environmental Sciences), the Bio21 Institute's Magnetic Resonance, and the Mass Spectrometry and Proteomics Facility (MSPF), Melbourne University are gratefully acknowledged.

Open access publishing facilitated by The University of Melbourne, as part of the Wiley - The University of Melbourne agreement via the Council of Australian University Librarians.

Conflict of Interest

The authors declare no conflict of interest.

Author Contributions

Joses G. Nathanael and **Haohan Kang** performed soil incubations. **Haohan Kang** synthesized DHB **12**. **Joses G. Nathanael** carried out the Michaelis–Menten kinetics. **Joses G. Nathanael** processed the experimental data and performed the analyses. **Uta Wille** performed the DFT calculations. **Joses G. Nathanael** and **Uta Wille** designed, planned, and supervised the work. All authors aided in interpreting the results. **Joses G. Nathanael** and **Uta Wille** wrote the manuscript and designed the figures with input from all authors.

© 2025 The Author(s). ChemPlusChem published by Wiley-VCH GmbH

Data Availability Statement

The data that support the findings of this study are available in the supplementary material of this article.

Keywords: density functional calculations · inhibition mechanism · inhibitors · N-(n-butyl)thiophosphoric triamide · soil incubation · urease

[1] United Nations, D. E. S. A., Population Division [online] **2022**, https://population.un.org/wpp/ (accessed: June 2023).
[2] W. M. Stewart, D. W. Dibb, A. E. Johnston, T. J. Smyth, *Agron. J.* **2005**, *97*, 1.
[3] W. M. Stewart, T. L. Roberts, *Proc. Engin* **2012**, *46*, 76.
[4] J. Penuelas, F. Coello, J. Sardans, *Agric. Food Secur.* **2023**, *12*, 5.
[5] FAO, FAOSTAT: Fertilizers by Nutrient, FAO.org [online] **2022**, https://www.fao.org/faostat/en/#data/RFN (accessed: June 2023).
[6] D. M. Huber, R. D. Watson, *Annu. Rev. Phytopathol.* **1974**, *12*, 139.
[7] K. Weber, M. Burow, *Physiol. Plant.* **2018**, *162*, 251,
[8] V. C. Baligar, N. K. Fageria, Z. L. He, *Commun. Soil Sci. Plan. Anal.* **2001**, *32*, 921.
[9] D. Chen, H. Suter, A. Islam, R. Edis, J. R. Freney, C. N. Walker, *Aust. J. Soil. Res.* **2008**, *46*, 289.
[10] K. C. Cameron, H. J. Di, J. L. Moir, *Ann. Appl. Biol.* **2013**, *162*, 145.
[11] X. Zhang, E. A. Davidson, D. L. Mauzerall, T. D. Searchinger, P. Dumas, Y. Shen, *Nature* **2015**, *528*, 51.
[12] T. M. Bowles, S. S. Atallah, E. E. Campbell, A. C. M. Gaudin, W. R. Wieder, A. S. Grandy, *Nat. Sustain.* **2018**, *1*, 399.
[13] J. W. Erisman, J. N. Galloway, S. Seitzinger, A. Bleeker, N. B. Dise, A. M. R. Petrescu, A. M. Leach, W. de Vries, *Philos. Trans. R. Soc. Lond. Ser. B.* **2013**, *368*, 20130116.
[14] L. A. Cox Jr, *Environ. Res.* **2023**, *223*, 115311.
[15] M. Insausti, R. Timmis, R. Kinnersley, M. C. Rufino, *Sci. Total Environ.* **2020**, *706*, 135124.
[16] S. Wang, J. Nan, C. Shi, Q. Fu, S. Gao, D. Wang, H. Cui, A. Saiz-Lopez, B. Zhou, *Sci. Rep.* **2015**, *5*, 15482.
[17] IFA, IFASTAT [Online] **2024**, https://www.ifastat.org/databases/plant-nutrition (accessed: May 2024).
[18] H. Cantarella, R. Otto, J. R. Soares, A. G. B. Silva, *J. Adv. Res.* **2018**, *13*, 19.
[19] B. Krawjewska, *J. Mol. Catal. B Enzym.* **2009**, *59*, 9.
[20] H. L. Mobley, R. P. Hausinger, *Microbiol. Rev.* **1989**, *53*, 85.
[21] N. von Wirén, A. Gojon, S. Chaillou, D. Raper, in *Plant Nitrogen* (Eds: P. J. Lea, J. F. Morot-Gaudry), Springer, Berlin, Heidelberg **2001**, pp. 61–77.
[22] A. F. Bouwman, L. J. M. Boumans, N. H. Batjes, *Global Biogeochem. Cycles* **2002**, *16*, 8.
[23] A. B. Llyod, M. J. Sheaffe, *Plant Soil* **1973**, *39*, 71.
[24] A. B. Mira, H. Cantarella, G. J. M. Souza-Netto, L. A. Moreira, M. Y. Kamogawa, R. Otto, *Agric. Ecosyst. Environ.* **2017**, *248*, 105.
[25] A. Sanz-Cobena, T. Misselbrook, V. Camp, A. Vallejo, *Atmos. Environ.* **2011**, *45*, 1517.
[26] W. Zhengping, O. van Cleemput, P. Demeyer, L. Baert, *Biol. Fertil. Soils* **1991**, *11*, 43.
[27] Y. Hu, U. Schmidhalter, *Environ. Res. Lett.* **2021**, *16*, 084047.
[28] S. Kiss, M. Simihaian, *Improving Efficiency of Urea Fertilizers by Inhibition of Soil Urease Activity*, 1st ed., Kluwer Academic Publishers, Dordrecht, The Netherlands **2002**, p. 3.
[29] W. H. R. Shaw, *J. Am. Chem. Soc.* **1954**, *76*, 2160.
[30] M. A. Tabatabai, *Soil Biol. Biochem.* **1977**, *9*, 9.
[31] J. Ashworth, H. M. Akerboom, J. M. Crépin, *Soil Sci. Soc. Am.* **1980**, *44*, 1247.
[32] J. M. Bremner, L. A. Douglas, *Soil Sci. Soc. Am.* **1973**, *37*, 225.
[33] K. B. Pugh, J. S. Waid, *Soil Biol. Biochem.* **1969**, *1*, 195.
[34] J. M. Bremner, L. A. Douglas, *Soil Biol. Biochem.* **1971**, *3*, 297.
[35] R. L. Mulvaney, J. M. Bremner, *Soil Biol. Biochem.* **1978**, *10*, 297.
[36] M. J. Domínguez, C. Sanmartin, M. Font, J. A. Palop, S. S. Francisco, O. Urrutia, F. Houdusse, J. M. García-Mina, *J. Agric. Food Chem.* **2008**, *56*, 3721.
[37] J. R. Simpson, J. R. Freney, W. A. Muirhead, R. Leuning, *Soil Sci. Soc. Am. J.* **1985**, *49*, 1426.
[38] B. Manunza, S. Deiana, M. Pintore, C. Gessa, *Soil Biol. Biochem.* **1999**, *31*, 789.
[39] A. G. B. Silva, C. H. Sequeira, R. A. Sermarini, R. Otto, *Agron. J.* **2017**, *109*, 1.
[40] C. D. L. Rawluk, C. A. Grant, G. J. Racz, *Can. J. Soil Sci.* **2001**, *81*, 239.
[41] G. Carmona, C. B. Christianson, B. H. Byrnes, *Soil Biol. Biochem.* **1990**, *22*, 933.
[42] R. Engel, C. Jones, R. Wallander, *Sci. Soc. Am. J.* **2011**, *75*, 2348.
[43] R. E. Engel, E. Williams, R. Wallander, J. Hilmer, *Sci. Soc. Am. J.* **2013**, *77*, 1424.
[44] J. M. Bremner, H. S. Chai, *Commun. Soil Sci. Plan. Anal.* **2008**, *17*, 337.
[45] S. S. Francisco, O. Urrutia, V. Martin, A. Persiteropoulos, J. M. Garcia-Mina, *J. Sci. Food Agric.* **2011**, *91*, 1569.
[46] E. Giannakis, J. Kushta, A. Bruggeman, J. Lelieveld, *Environ. Sci. Eur.* **2019**, *31*, 93.
[47] B. Gu, L. Zhang, R. van Dingenen, M. Vieno, H. J. M. van Grinsven, X. Zhang, S. Zhang, Y. Chen, S. Wang, C. Ren, S. Rao, M. Holland, W. Winiwarter, D. Chen, J. Xu, M. A. Sutton, *Science* **2021**, *374*, 758.
[48] L. G. Bundy, J. M. Bremner, *Soil Biol. Biochem.* **1973**, *5*, 847.
[49] L. Mazzei, M. Cianci, F. Musiani, G. Lente, M. Palombo, S. Ciurli, *J. Inorg. Biochem.* **2017**, *166*, 182.
[50] L. Mazzei, U. Contaldo, F. Musiani, M. Cianci, G. Bagnolini, M. Roberti, S. Ciurli, *Angew. Chem., Int. Ed.* **2021**, *60*, 6029.
[51] D. J. Kahl, K. M. Hutchings, E. M. Lisabeth, A. J. Haak, J. R. Leipprandt, T. Dexheimer, D. Khanna, P.-S. Tsou, P. L. Campbell, D. A. Fox, B. Wen, D. Sun, M. Bailie, R. R. Neubig, S. D. Larsen, *J. Med. Chem.* **2019**, *62*, 4350.
[52] A. O. Luchibia, H. Suter, H.-W. Hu, S. K. Lam, J.-Z. He, *J. Soil. Sediment.* **2020**, *20*, 1309.
[53] D. M. Linn, J. W. Doran, *Soil Sci. Soc. Am. J.* **1984**, *48*, 1267.
[54] S. K. Lam, H. Suter, M. Bai, C. Walker, R. Davies, A. R. Mosier, D. Chen, *Sci. Total Environ.* **2018**, *644*, 1531.
[55] M. W. Weatherburn, *Anal. Chem.* **1967**, *39*, 971.
[56] M. J. Frisch, G. W. Trucks, H. B. Schlegel, G. E. Scuseria, M. A. Robb, J. R. Cheeseman, G. Scalmani, V. Barone, G. A. Petersson, H. Nakatsuji, X. Li, M. Caricato, A. V. Marenich, J. Bloino, B. G. Janesko, R. Gomperts, B. Mennucci, H. P. Hratchian, J. V. Ortiz, A. F. Izmaylov, J. L. Sonnenberg, D. Williams-Young, F. Ding, F. Lipparini, F. Egidi, J. Goings, B. Peng, A. Petrone, T. Henderson, D. Ranasinghe, V. G. Zakrzewski, J. Gao, N. Rega, G. Zheng, W. Liang, M. Hada, M. Ehara, K. Toyota, R. Fukuda, J. Hasegawa, M. Ishida, T. Nakajima, Y. Honda, O. Kitao, H. Nakai, T. Vreven, K. Throssell, J. A. Montgomery, J. E. Peralta, F. Ogliaro, M. J. Bearpark, J. J. Heyd, E. N. Brothers, K.N. Kudin, V. N. Staroverov, T. A. Keith, R. Kobayashi, J. Normand, K. Raghavachari, A. P. Rendell, J. C. Burant, S. S. Iyengar, J. Tomasi, M. Cossi, J. M. Millam, M. Klene, C. Adamo, R. Cammi, J. W. Ochterski, R. L. Martin, K. Morokuma, O. Farkas, J. B. Foresman, D. J. Fox, *Gaussian 16, Revision C.01*, Gaussian, Inc., Wallingford, CT **2016**, GaussView 5.0. Wallingford, E.U.A.
[57] Y. Zhao, D. G. Truhlar, *Theor. Chem. Acc.* **2008**, *120*, 215.
[58] R. A. Kendall, T. H. Dunning, *J. Chem. Phys.* **1992**, *96*, 6796.
[59] Y. Takano, K. N. Houk, *J. Chem. Theory Comput.* **2005**, *1*, 70.
[60] S. Grimme, J. Antony, S. Ehrlich, H. Krieg, *J. Chem. Phys.* **2010**, *132*, 154104.
[61] M. I. Zantua, L. C. Dumenil, J. M. Bremner, *Soil Sci. Soc. Am. J.* **1977**, *41*, 350.
[62] J. Strelow, W. Dewe, P. W. Iversen, H. B. Brooks, J. A. Radding, J. McGee, J. Weidner, in *Mechanism of Action Assays for Enzymes in: Assay Guidance Manual* (Eds: S. Markossian, A. Grossman, M. Arkin, et al.), [Internet: 2012 May 1, Updated 2012 October 1], Eli Lilly & Company and the National Center for Advancing Translational Sciences, Bethesda, MD **2004**. https://www.ncbi.nlm.nih.gov/books/NBK92001 (accessed: July 2024).
[63] M. P. Byrne, J. T. Tobin, P. J. Forrestal, M. Danaher, C. G. Nkwonta, K. Richards, E. Cummins, S. A. Hogan, T. F. O'Callaghan, *Sustainability* **2020**, *12*, 6018.
[64] D. R. Lide, *CRC Handbook of Chemistry and Physics*, 87th ed., CRC Press, Boca Raton, FL **2006**, ISBN 0-8493-0487-3.
[65] M. Lucarini, G. F. Pedulli, M. Guerra, *Chem. Eur. J.* **2004**, *10*, 933.
[66] P. C. Jocelyn, *Eur. J. Biochem.* **1967**, *2*, 327.
[67] M. L. Colarieti, G. Toscano, M. R. Ardi, *J. Hazard. Mater.* **2006**, *134*, 161.
[68] M. L. Alfieri, A. Cariola, L. Panzella, A. Napolitano, M. d'Ischia, L. Valgimigli, O. Crescenzi, *J. Org. Chem.* **2022**, *87*, 4580.
[69] T. K. Harris, G. J. Turner, *IUBMB Life* **2022**, *53*, 85.
[70] L. Mazzei, M. Cianci, U. Contaldo, S. Ciurli, *J. Agric. Food Chem.* **2019**, *67*, 2127.
[71] TFI, What are the 4Rs? [online], https://www.tfi.org/insights/nutrient-stewardship/what-are-the-4rs/ (accessed: June 2025).

Manuscript received: February 3, 2025
Version of record online: June 20, 2025

© 2025 The Author(s). ChemPlusChem published by Wiley-VCH GmbH